ACS APPLIED POLYMER MATERIALS

Forum Article

Cite This: ACS Appl. Polym. Mater. 2020, 2, 40−54

pubs.acs.org/acsapm

Anomalous, Multistage Liquid Water Diffusion and Ionomer Swelling Kinetics in Nafion and Nafion Nanocomposites

Apoorv Balwani and Eric M. Davis*

Department of Chemical and Biomolecular Engineering, Clemson University, Clemson, South Carolina 29634, United States

Supporting Information

ABSTRACT: The advent of commercially viable vanadium redox flow batteries has generated interest in improving upon existing membrane materials utilized in this grid-scale energy storage technology. Elucidating structure−transport relationships in perfluorosulfonated ionomer nanocomposites is of particular importance for the development of next-generation membranes, as there is a limited understanding of how nanoparticles alter transport in these membranes. In the present study, we attempt to resolve the impact of silica nanoparticles (SiNPs) on liquid water transport in Nafion−SiNP membranes. Specifically, liquid water sorption and ionomer swelling kinetics in a series of Nafion−SiNP membranes were evaluated using time-resolved attenuated total reflectance−Fourier transform infrared spectroscopy. Anomalous, multistage water uptake and swelling kinetics were observed for both Nafion and Nafion−SiNP membranes at all SiNP loadings. The first stage of the kinetic data was regressed to a diffusion−relaxation model, as water diffusion and resulting diffusion-induced polymer relaxation kinetics during this first stage were found to be highly coupled. Suppressed water transport and swelling kinetics were observed with the introduction of SiNPs, though this trend did not hold true for higher SiNP loadings. Thermal annealing of the membranes was also observed to impact the transport and swelling properties of the Nafion and Nafion−SiNP membranes, exhibiting a synergistic effect with the SiNPs at low nanoparticle loadings. Finally, the multistage water uptake mechanism in dry Nafion and Nafion−SiNP nanocomposites was understood to be governed by the time-dependent local water activity in the membrane. Overall, this study presents a clear framework that can be employed to characterize and tune aqueous transport through Nafion nanocomposite membranes.

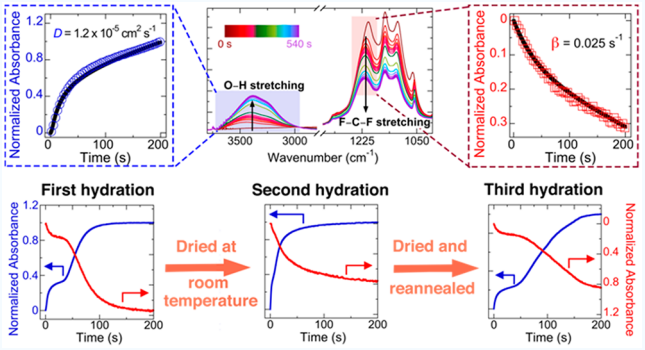

KEYWORDS: *Nafion nanocomposites, water diffusion, polymer relaxation, vanadium redox flow battery, membranes*

INTRODUCTION

Vanadium redox flow batteries (VRFBs) are a promising large-scale energy storage technology due to their robustness, flexible design, and high energy density.[1] The current state-of-the-art ionomer utilized in these flow batteries, Nafion, is a perfluorosulfonic acid polymer which, when hydrated, nanophase segregates into an interconnected network of sulfonic acid-lined ionic channels within a cocontinuous hydrophobic matrix of fluorocarbon backbone chains. These ionic channels are excellent conduits for proton transport across the ionomer (proton conductivity of Nafion ≈ 10^{-1} S cm^{-1}), while the Teflon-like matrix provides excellent thermochemical stability, making Nafion ideal for use in the acidic, aqueous environment of the redox flow battery.[2,3]

However, a long-standing issue with the use of Nafion in these redox flow batteries is the high rate at which vanadium ions cross over from the anolyte to the catholyte (and vice versa). This undesired crossover results in reduced performance and lifetime of VRFBs, which has prevented the widespread adoption of this technology.[1,2,4,5] To date, numerous strategies to counter the poor ion selectivity of Nafion have been explored,[5] though many of these approaches are not ideal for practical implementation as the chemical modifications result in an undesirable reduction in proton conductivity or loss of chemical robustness of the resulting membrane. Further, some of these fabrication methods present challenges with regard to commercial scale-up.

In contrast, incorporation of silica nanoparticles (SiNPs) into the ionomer, which was previously found to result in excellent methanol crossover resistance,[6−9] has emerged as a promising strategy to combat the high vanadium ion crossover observed in Nafion, with neither significantly suppressing membrane performance or being too cost-inhibitive.[2,4,5,10] Nafion nanocomposites (referred to as Nafion−SiNP membranes) traditionally have been fabricated via an in situ sol-gel condensation process, whereby the silica phase is formed

Special Issue: Young Investigator Forum

Received: September 16, 2019
Accepted: November 11, 2019
Published: December 13, 2019

DOI: 10.1021/acsapm.9b00866
ACS Appl. Polym. Mater. 2020, 2, 40−54

directly within a preformed (i.e., extruded) Nafion membrane (e.g., Nafion 117).[2,5,8,9] Additionally, but far less frequently, these nanocomposites have been fabricated using a solution-cast process, where a dispersion of preformed, discrete nanoparticles and Nafion is cast onto a substrate, and the solvent is allowed to evaporate, forming a dense membrane.[6,10] Both fabrication methods produce composite membranes that exhibit reduced permeability of vanadium ions (when compared to their unmodified counterpart, i.e., Nafion containing no SiNPs). Until recently, this reduction in vanadium ion permeability has been attributed to the presence of SiNPs within the ionic channels in Nafion, where the nanoparticles (NPs) are posited to inhibit the crossover of vanadium ions due to a size-exclusion mechanism.[5,9] However, recent small-angle X-ray and neutron scattering experiments on Nafion−SiNP membranes fabricated via sol-gel condensation show that these nanoparticles are too large to solely reside within the ionic channels.[2] These recent investigations underscore our lack of understanding regarding how the introduction of NPs reduces the transport of vanadium ions across the membrane.

To this end, it is also paramount that we better understand how factors such as water dynamics and ionomer chain mobility are impacted by the introduction of NPs, as both are known to influence the overall transport properties of the polymer.[11−13] The impact of NPs on the local polymer segmental mobility has been well documented in literature. Most notably, it has been shown that the presence of NPs alters the dynamics of the polymer chains directly adjacent to the NP surface, known as the "bound layer". These dynamics have been probed through various thermomechanical, electrochemical, and vibrational spectroscopy studies[14] as well as with quasi-elastic neutron scattering. In the latter, Gagliardi and coworkers[15] directly quantified the reduction in mobility of chain segments in poly(dimethylsiloxane) and poly(vinyl acetate) filled with fumed SiNPs. They reported the existence of two separate dynamic processes in the nanocomposites, where they attribute the slower dynamic mode to suppressed chain dynamics near the polymer−SiNP interface.

Of direct relevance to the current investigation, recent studies on Nafion thin films suggest that both nanophase ordering and segmental dynamics of the ionomer are affected by the hydrophilic nature of the ionomer−substrate interface,[16−18] lending credence to the idea that ionomer−SiNP interactions impact the segmental dynamics near the ionomer−SiNP interface. More recently, our group investigated the hydrated relaxation dynamics of both sol-gel and solution-cast Nafion and Nafion−SiNP membranes. In that study, time-resolved attenuated total reflectance-Fourier transform infrared (*t*ATR-FTIR) spectroscopy and neutron spin echo (NSE) spectroscopy were used to characterize water sorption-induced swelling kinetics and local chain relaxation dynamics, respectively.[19] Suppressed local segmental dynamics and suppressed bulk swelling kinetics were observed for both sol-gel and solution-cast Nafion−SiNP membranes at low SiNP loadings (∼4 wt %). Surprisingly, when the SiNP loading was increased (∼10 wt %), an enhancement in both the local and bulk dynamics of the sol-gel Nafion−SiNP membranes was observed.

In addition to aforementioned literature regarding the impact of NPs/interfaces on polymer segmental dynamics, water transport in Nafion has been thoroughly investigated, as the behavior and amount of water (i.e., hydration level) in these ionomer membranes regulates the overall membrane transport properties (e.g., ion conductivity and permselectivity).[11] The hydration level is also seen to directly impact the ionomer segmental dynamics, as water plasticizes the ionomer, leading to increased dynamics in hydrated membranes.[12] With regards to water uptake kinetics, the transport of both liquid water and water vapor through extruded Nafion membranes is found to be limited by the rate of polymer swelling.[20] Liquid water transport through Nafion was observed to be significantly faster than that of water vapor (presented as a case for Schroeder's paradox).[21] Furthermore, the mechanism of the water transport (i.e., Fickian vs non-Fickian) has been shown to depend on the water activity with which the membrane is challenged.[22] While there is a large body of work in the literature regarding water vapor transport in Nafion membranes,[20,22−28] investigations of liquid water transport in Nafion and Nafion nanocomposites are far less prevalent. As both the thermal treatment and the introduction of SiNPs are understood to affect the structure and viscoelastic properties of hydrated Nafion nanocomposites,[7,10,16−18,29−34] a thorough investigation is needed to help elucidate the exact mechanism by which the SiNPs alter water transport in these ionomer nanocomposites.

Herein, for the first time, we employ *t*ATR-FTIR spectroscopy to characterize liquid water transport in a series of solution-cast Nafion and Nafion−SiNP membranes. The silica content in each membrane was varied between 0 wt % (i.e., no SiNPs) and 10 wt %. Unlike traditional techniques used to capture aqueous transport in polymer membranes (e.g., "pat-and-weigh" method), *t*ATR-FTIR spectroscopy provides molecular-level resolution of both the nanocomposite and water, allowing for simultaneous tracking of changes in the water concentration (diffusion) as well as ionomer chain rearrangements (swelling). Furthermore, this experimental technique has been previously utilized to investigate solvent transport in various polymer nanocomposites and has yielded useful insights into the mechanisms by which NPs disrupt native transport behavior.[35,36] The *t*ATR-FTIR water uptake data were regressed to a coupled diffusion−relaxation model, where both a polymer relaxation time constant (β) and the mutual diffusion coefficient of water through Nafion (D) were calculated. The values of D and β allude to the impact of thermal treatment and incorporation of SiNPs on the viscoelastic and water transport properties of these nanocomposites.

EXPERIMENTAL SECTION

Materials. Nafion perfluorinated resin solution (20 wt % in mixture of lower aliphatic alcohols and water, equivalent weight = 1100 g/mol sulfonic acid) and deuterium oxide (D_2O, 99.9 atom % D) were purchased from Sigma-Aldrich. Silica nanoparticles (99.5% purity, 10 to 20 nm particle size, nonporous) were obtained from Nissan Chemicals as a dispersion in methanol (30 wt % silica). Additionally, deionized (DI) water (resistivity ≈ 18 MΩ·cm) and dry, high-purity nitrogen gas were used for all liquid water transport experiments.

Preparation of Solution-Cast Nafion−SiNP Membranes. A series of Nafion−SiNP membranes (silica content varying from 0 to 10 wt %) was synthesized as follows. The as-received Nafion stock solution was transferred into a 25 mL scintillation vial and weighed, and the appropriate amount of SiNPs (based on the mass of Nafion) was added to the solution. The vials were sonicated for 3−4 h to ensure uniform mixing of the SiNPs in solution. Following this, the dispersions were immediately cast onto a trapezoidal, multireflection

DOI: 10.1021/acsapm.9b00866
ACS Appl. Polym. Mater. 2020, 2, 40−54

germanium (Ge) ATR crystal and allowed to dry in the air at room temperature overnight. For membranes requiring thermal treatment, the polymer-coated crystals were annealed at 140 °C for 2 h under dynamic vacuum. After 2 h, the oven was shut off, and the films were allowed to slowly cool to room temperature under static vacuum. Once cooled, the ionomer-coated ATR crystals were placed in a desiccator until liquid water transport experiments were performed. Note, the term "wt %" indicates the ratio of the mass of silica to the mass of Nafion (i.e., g SiO_2/g Nafion).

***t*ATR-FTIR Spectroscopy.** For liquid water diffusion measurements, time-resolved IR spectra were collected using a FT-IR spectrometer (Nicolet iS50R FT-IR spectrometer; Thermo Scientific) coupled with horizontal, temperature-controlled ATR cell (Gateway ATR accessory; Specac, Inc.). Data collection was done using a liquid nitrogen-cooled mercury−cadmium−telluride (MCT) detector at a rate of 2 scans per spectrum and a resolution of 4 cm^{-1}, resulting in a repeat collection time of ≈0.78 s for *t*ATR-FTIR experiments.

Prior to depositing the dispersions onto the ATR crystal, the background spectrum of a clean (bare) ATR crystal (i.e., uncoated) was collected, and all subsequent spectra collected during the experiment were subtracted from this spectrum. Solution-cast membranes were deposited onto a multiple reflection, trapezoidal germanium (Ge) ATR crystal (Specac, Inc., 45° beveled faces) as previously described. Next, the ionomer-coated ATR crystal was placed face down into the flow-through cell, and the back plate was tightened down on the backside of the crystal. Note, a Kalrez gasket was used between the top-plate and the top side of the film to ensure proper sealing during transport experiments. The cell was then mounted on the ATR accessory, and the films were dried under dry, high-purity nitrogen flow for approximately 4 h before beginning each experiment.

Liquid water diffusion experiments were initiated by introducing deionized water into the space above the polymer film ($V \approx 550\ \mu L$; the side opposite the polymer−crystal interface) in the ATR cell. To prevent evaporation during the experiment, the inlet and outlet of the flow-through cell were sealed using Parafilm. All spectra were collected at a temperature of 25 °C, which was maintained using a circulating temperature bath. Immediately following each experiment, the thickness of the hydrated membranes was measured using a digital micrometer (Mitutoyo) with an accuracy of 1 μm. The reported value of film thickness is averaged from five individual measurements at different positions along the length of the film. A detailed schematic of this experimental setup is provided in Figure S1 of the Supporting Information.

In this experiment, transient Fickian diffusion kinetics of water through the Nafion−SiNP membranes can be described by the one-dimensional continuity equation (Fick's second law);

$$\frac{\partial C}{\partial t} = D\frac{\partial^2 C}{\partial z^2} \tag{1}$$

where C is the concentration of water, t is time, z is the distance across the film ($z = 0$ at polymer−ATR interface), and D is the mutual diffusion coefficient of water in the polymer. For one-dimensional (rectangular geometry) water transport through a Nafion membrane of thickness L, the initial condition and boundary conditions are as follows

$$C = C_0 \text{ at } 0 < z < L \text{ and } t = 0 \tag{2}$$

$$C = C_L \text{ at } z = L \text{ and } t \geq 0 \tag{3}$$

$$\frac{dC}{dz} = 0 \text{ at } z = 0 \text{ and } t \geq 0 \tag{4}$$

where C_0 is the initial concentration of water inside the membrane (zero for this study), and C_L is the concentration of water at the membrane surface. The coordinates were chosen so that $z = 0$ is the ionomer−crystal interface and $z = L$ is the ionomer−water interface. Using the above initial and boundary conditions, the analytical solution of eq 1 is given as

$$\frac{C(t) - C_0}{C_{eq} - C_0} = 1 - \frac{4}{\pi}\sum_{n=0}^{\infty}\frac{(-1)^n}{(2n+1)}\exp(-Df^2 t)\cos(fz), \quad \text{where } f = \frac{(2n+1)\pi}{2L}, \tag{5}$$

where $C(t)$ and C_{eq} are the concentration of water at any time t and the final water concentration inside the membrane, respectively. The experimental IR absorbance of a species can be related to the concentration of that species by making use of the differential form of the Beer−Lambert law, which is given as

$$A = \int_0^L \varepsilon^* C(t)\exp\left(\frac{-2z}{d_p}\right)dz \tag{6}$$

where A is the ATR absorbance value, ε^* is the molar extinction coefficient (which can be considered constant under the assumption of weak IR absorbance), and d_p is the depth of penetration of the evanescent wave at the polymer−ATR crystal interface and is a function of refractive indices of the polymer and the crystal. For this study, $d_p \approx 1\ \mu m$. Substituting eq 5 into eq 6 and integrating results in the following

$$\frac{A(t) - A_0}{A_{eq} - A_0} = 1 - \left[\frac{8}{\pi d_p\left(1 - \exp\left(\frac{-2L}{d_p}\right)\right)}\right] \times \sum_{n=0}^{\infty}\frac{1}{(2n+1)}\left[\frac{\exp(-Df^2 t)\left[f\exp\left(\frac{-2L}{d_p}\right) + (-1)^n\left(\frac{2}{d_p}\right)\right]}{\left(\frac{2}{d_p}\right)^2 + f^2}\right] \tag{7}$$

where $A(t)$, A_0, and A_{eq} are the ATR absorbance values at any time t, at $t = 0$, and at equilibrium, respectively. Note, for these experiments, the film thicknesses were, on average, two orders of magnitude larger than the depth of evanescent wave penetration (≈100 μm vs ≈1 μm). As such, eq 7 can be simplified using the thick film approximation ($L/d_p \gg 10$), resulting in the following equation

$$\frac{A(t) - A_0}{A_{eq} - A_0} = 1 - \frac{4}{\pi}\sum_{n=0}^{\infty}\frac{(-1)^n}{(2n+1)}\exp(-Df^2 t) \tag{8}$$

The diffusion of water into the ionomer membrane exerts an osmotic stress on the ionic channels, resulting in diffusion-driven polymer swelling.[25,26,29,39−41] The swelling kinetics of the membrane can be modeled using the following three-element viscoelastic model

$$\varepsilon \approx \frac{A_0}{A(t)} - 1 = \frac{\sigma_0}{\eta}t + \frac{\sigma_0}{E}(1 - \exp(-\beta t)) \tag{9}$$

where σ_0, ε, η, E, and β are the stress, strain, dynamic viscosity, Young's modulus, and relaxation time constant, respectively. We have previously described, in depth, the treatment of ionomer swelling kinetics with this model.[20] The liquid water uptake data can be modeled by combining eq 9 with eq 8, forming the following coupled diffusion−relaxation model

$$\frac{A - A_0}{A_{eq} - A_0} = F_A\left[1 - \frac{4}{\pi}\sum_{n=0}^{\infty}\frac{(-1)^n}{(2n+1)}\exp(-Df^2 t)\right] + F_B\left[w_2\frac{t}{t_f} + w_1(1 - \exp(-\beta t))\right] \tag{10}$$

where $w_1 = \frac{\eta/E}{t_f + \eta/E}$ and, $w_2 = \frac{t_f}{t_f + \eta/E}$

Here, w_1 and w_2 arise from the normalization of eq 9, while F_A and F_B are weighting fractions which indicate the contributions of the Fickian

DOI: 10.1021/acsapm.9b00866
ACS Appl. Polym. Mater. 2020, 2, 40−54

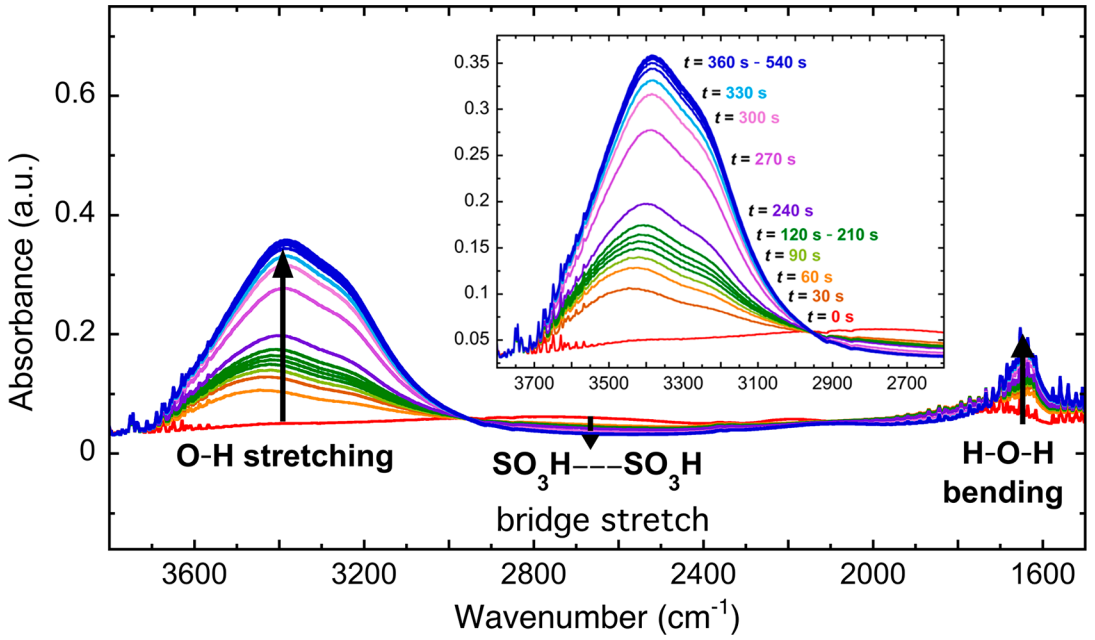

Figure 1. Time-resolved ATR-FTIR spectra of liquid water diffusion in an initially dry, annealed Nafion membrane containing 4 wt % SiNPs at 25 °C. The arrows indicate the direction of spectral change with time.

diffusion and polymer swelling, respectively, on the overall water sorption kinetics. The time-resolved sorption data can then be regressed to eq 10, with the water diffusion coefficient, D, as the only adjustable parameter.

RESULTS

As seen in Figure 1, two new spectral bands appear as water diffuses through the initially dry ionomer nanocomposite and accumulates at the polymer−ATR crystal interface. The smaller infrared peak centered around 1640 cm^{-1} can be assigned to the water H−O−H bending vibrational mode, while the broad infrared band that emerges at higher wavenumbers can be assigned to the O−H stretching of water.[42] The inset in Figure 1 shows an enlarged image of the time-resolved O−H stretching region. The time points associated with each spectrum are listed to the right of the O−H stretching peak. Upon further investigation of the time-resolved O−H spectra, there appear to be two distinct regions (or stages) of water diffusion in the ionomer nanocomposite. Focusing on the spectral data from t = 0 to 210 s, we observe an initial, fast increase in the area of the O−H stretching peak (t = 0 to 90 s). After this initial, fast increase, the growth of the O−H stretching peak slows significantly, where there is little change observed in the area of this peak from t = 120 to 210 s (shown as dark green spectra in Figure 1). However, after t = 210 s, there is another fast increase in the growth of the O−H stretching peak (t > 210 s), followed by a slow approach to equilibrium over t = 360 to 540 s (shown as dark blue spectra in Figure 1).

The water uptake kinetics in the Nafion membrane containing 4 wt % SiNPs can be determined by measuring the area under this peak (in this case, from 3774 to 2874 cm^{-1}) as a function of time. This analysis was performed, and the results are presented in Figure 2. As seen from Figure 2, a two-stage uptake process is observed as liquid water diffuses into the initially dry nanocomposite membrane. Note, analogous multistage water uptake curves were obtained for all Nafion and Nafion−SiNP membranes. The water uptake and swelling

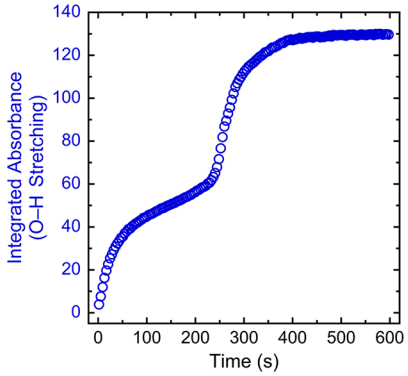

Figure 2. Integrated absorbance of the O−H stretching infrared band as a function of time for liquid water diffusion in annealed Nafion containing 4 wt % SiNPs at 25 °C. Note, only 20% of the data are shown for clarity.

kinetic data for each membrane can be found in Figures S2−S6 in the Supporting Information.

To our knowledge, this is the first time that a multistage liquid water diffusion process in Nafion and/or Nafion nanocomposites has been observed. However, the presence of a two-stage water sorption process in extruded Nafion has been previously postulated.[26] In that study, the investigators noted the presence of a distinct transition in values of ionic channel tortuosity, membrane free volume, and water self-diffusivity with increasing water activity inside the membrane. Specifically, this transition was observed at a hydration number (λ; number of water molecules per sulfonic group) of $\lambda \approx 4$. This led the investigators to conjecture that hydration of the extruded ionomer can be mechanistically broken down into two steps: (1) the formation of a primary hydration shell around the sulfonic groups, where diffusing water molecules work against local rearrangements of the collapsed ionic network, which is followed by (2) the formation of the fully hydrated ionic network, whereby the flux of water is governed by the relaxation of the hydrophobic matrix. While the specific

DOI: 10.1021/acsapm.9b00866
ACS Appl. Polym. Mater. 2020, 2, 40−54

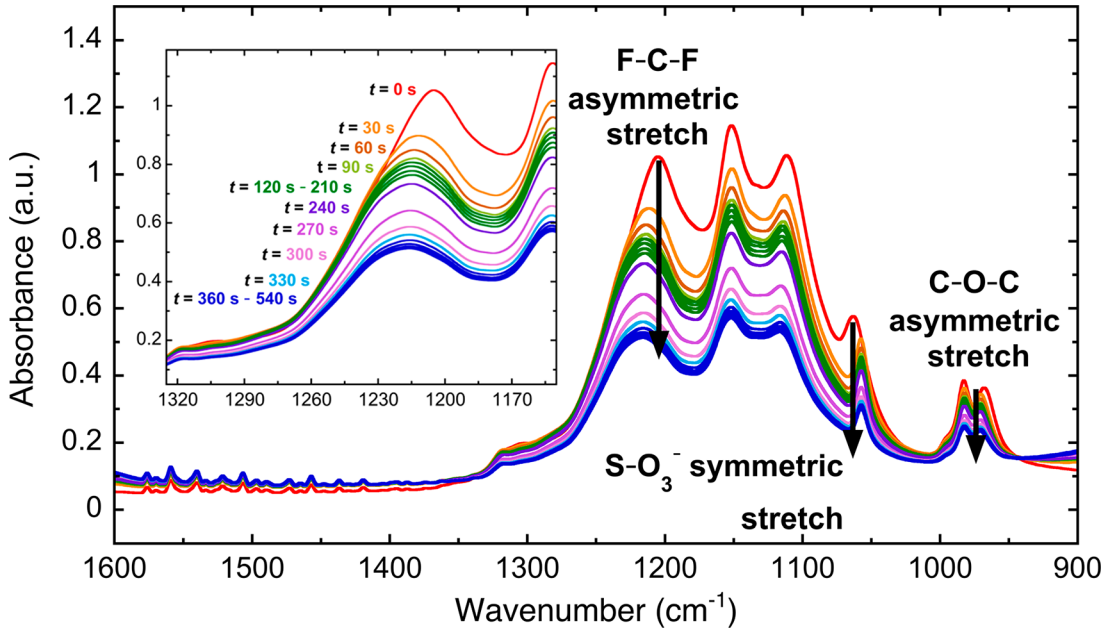

Figure 3. Time-resolved infrared spectra of the polymer fingerprint region for liquid water diffusion in annealed Nafion containing 4 wt % SiNPs at 25 °C, where arrows indicate the direction of spectral change with time. The inset shows a more resolved picture of evolution of F−C−F asymmetric stretching peak, where the color-coded time points associated with each spectrum are shown to the left of the F−C−F peak.

multistage liquid water kinetics reported here have not been previously observed, anomalous water transport in Nafion, both bulk membranes (>1 μm) and thin films (<500 nm), has been previously reported.[23,25,26,29,39−41,43] Of particular relevance to this study, a recent investigation using *t*ATR-FTIR spectroscopy to capture water vapor diffusion in Nafion noted that the Fickian nature of water transport through the ionic channels is affected by changes to the channel geometry due to the diffusion-driven polymer swelling of the ionomer.[23] As a result, changes to the time-resolved O−H stretching spectra are impacted by the swelling kinetics of the ionomer, which occur on a similar time scale as water diffusion.

To investigate the relationship between liquid water diffusion and the swelling kinetics of the ionomer nanocomposite, we turn to the polymer fingerprint region of the spectrum. As *t*ATR-FTIR spectroscopy simultaneously provides molecular-level information about the penetrant (in this case water) and the polymer (in this case the Nafion nanocomposite) during water transport experiments, it allows us to discern the associated processes (i.e., penetrant diffusion and polymer swelling) in real time. Figure 3 shows the time-resolved ATR-FTIR spectra of the fingerprint region (between 1350 and 900 cm^{-1}) for Nafion during the diffusion of liquid water into ionomer nanocomposite. The two infrared bands located at approximately 1210 and 1160 cm^{-1} can be assigned to the asymmetric and symmetric fluorocarbon (F−C−F) stretching modes, respectively. The infrared band located at ≈1060 cm^{-1} can be assigned to the SO_3^- symmetric stretching, while the two infrared bands located at ≈982 and ≈966 cm^{-1} can be assigned to the C−O−C asymmetric and symmetric stretching, respectively. The infrared signal arising from asymmetric F−C−F stretching of the fluorocarbon chains in the Nafion backbone[44] can be used to track changes in the swelling behavior of the hydrophilic ionic network. The inset in Figure 3 shows a more resolved picture of evolution of this peak with time, where the time points associated with each spectrum are noted on the left.

In Figure 3, diffusion-driven polymer swelling is manifested as a decrease in absorbance of these infrared bands with time. Similar to the time-resolved spectra shown in Figure 1, the decrease in intensity of the F−C−F stretching infrared band appears to occur in two distinctly separate stages. The swelling kinetics of the ionomer nanocomposite can be determined by calculating the area under this infrared band as a function of time. This analysis was performed, and the normalized swelling kinetic data are shown in Figure 4 (open red squares). Note, as

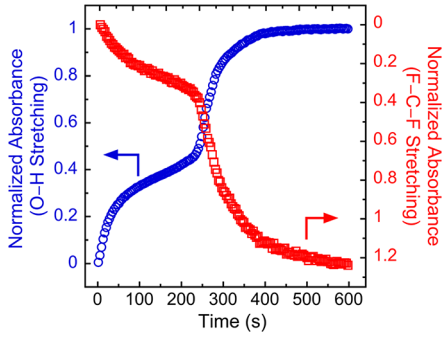

Figure 4. Time-resolved, normalized F−C−F stretching absorbance data (open red squares) of annealed Nafion containing 4 wt % SiNPs at 25 °C. The time-resolved, normalized O−H stretching kinetic data (open blue circles) have also been included to highlight the coupled nature of water diffusion and polymer relaxation (or swelling) kinetics. Note, only 20% of the data are shown for the sake of clarity.

the F−C−F stretching absorbance data have been normalized as $(A_0/A(t)) - 1$ (see Experimental Section), these data have been plotted in reverse order on the right *x*-axis (colored red in Figure 4 to better mimic the decrease in absorbance observed in the time-resolved spectra shown in Figure 3. Further, the time-resolved O−H stretching absorbance data from Figure 2 have been normalized and also plotted in Figure 4 (open blue circles). The water-induced swelling kinetics confirm the two-

DOI: 10.1021/acsapm.9b00866
ACS Appl. Polym. Mater. 2020, 2, 40−54

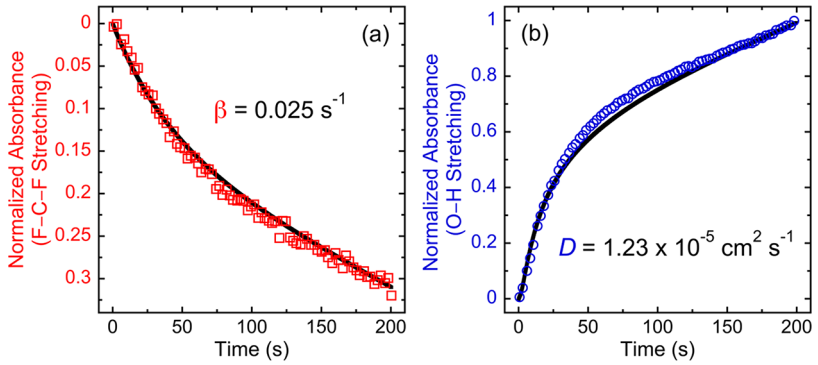

Figure 5. (a) Time-resolved, normalized F−C−F stretching absorbance data (open red squares) of annealed Nafion containing 4 wt % SiNPs at 25 °C. The solid black line represents the best-fit regression of the three-element viscoelastic relaxation model (eq 9), where the relaxation time constant, β, was the only adjustable parameter. (b) Time-resolved, normalized O−H stretching absorbance data (open blue circles) of annealed Nafion containing 4 wt % SiNPs at 25 °C. The solid black line represents the best-fit regression of the diffusion−relaxation model (eq 10), where the water diffusion coefficient, D, was the only adjustable parameter. Note, only 30% of the data is shown for clarity.

Table 1. Normalized Relaxation Time Constants, Water Diffusion Coefficients, and Diffusional Deborah Numbers for Solution-Cast Nafion and Nafion−SiNP Membranes[a]

Membrane	Range of film thicknesses (L, μm)	Normalized relaxation time constant (β_{norm}, 10^{-6} cm^2 s^{-1})	Water diffusion coefficient (D, 10^{-6} cm^2 s^{-1})	Deborah number (De, −)
		Unannealed		
Nafion (0 wt % SiO_2)	69−150	4.6 ± 0.4	8.3 ± 1.6	1.8 ± 0.4
Nafion−SiNP (4 wt % SiO_2)	150−238	11.8 ± 6.2	16.6 ± 3.9	1.4 ± 0.4
		Annealed		
Nafion (0 wt % SiO_2)	170−189	19.3 ± 2.5	22.4 ± 4.3	1.2 ± 0.1
Nafion−SiNP (4 wt % SiO_2)	150−196	9.2 ± 4.3	5.7 ± 2.4	0.7 ± 0.3
Nafion−SiNP (10 wt % SiO_2)	237−270	26.2 ± 11.2	19.3 ± 6.3	0.8 ± 0.3

[a]Note, the values listed in the table are an average of multiple (at least three) experiments, and the ± values represent the standard deviation of the calculated, averaged parameter.

stage relaxation process that was seen in the time-resolved IR spectra shown in the inset in Figure 3. Further, it is clear from Figure 4 that water diffusion and diffusion-induced polymer swelling in these ionomer nanocomposites are strongly coupled.

The presence of a multistage relaxation process during liquid water hydration has been previously observed by our group.[20] In that study, a three-element viscoelastic model was regressed to the first stage of the diffusion-induced polymer relaxation ($0 \leq t \leq 100$ s) to obtain a relaxation time constant (β), as regression of the model to the entire data set ($t > 100$ s) yielded a poor fit. Therein, an increase in the relaxation time constant was seen in the "short time" time-resolved absorbance data when compared to the time constant obtained when the entire data set was fit, suggesting that polymer relaxation occurring at various time scales originates from short-time polymer reorganization taking place due to the hydration of an initially dry membrane. Similar results have been reported with experiments using time-resolved small-angle X-ray scattering experiments during liquid water sorption,[45] time-resolved small-angle neutron scattering experiments during water vapor sorption,[29] and contact angle measurements during liquid water sorption in dry Nafion films,[46] where at least two distinct regimes of water sorption and polymer relaxation were observed at similar time scales as those presented here.

To gain a more quantitative measure of the two-stage polymer swelling kinetics and liquid water diffusivity in these membranes, the first stages of the time-resolved F−C−F and O−H stretching IR data were analyzed using a three-element viscoelastic model and a diffusion−relaxation model, respectively. Figure 5a shows the results of the regression of the three-element viscoelastic relaxation model (solid black line, eq 9) to the time-resolved, normalized F−C−F stretching data (open red squares), where the relaxation time constant, β, was the only adjustable parameter. As seen from Figure 5a, the viscoelastic model (solid black line) accurately captures the swelling kinetics of the Nafion−SiNP membrane, where a relaxation time constant of $\beta = 0.025$ s^{-1} was obtained. Next, the relaxation model parameters obtained from this regression were fed into the polymer swelling-adjusted diffusion model (eq 10),[23] leaving the water diffusion coefficient D as the only adjustable parameter. Figure 5b shows the results of the regression of the diffusion−relaxation model (solid black line, eq 10) to the time-resolved O−H stretching data (open blue circles). As seen from Figure 5b, the diffusion−relaxation model accurately captures the liquid water sorption kinetics of the Nafion nanocomposite membrane, where a diffusion coefficient of $D = 1.23 \times 10^{-5}$ cm^2 s^{-1} was obtained. This analysis was extended to unmodified Nafion (i.e., Nafion with no SiNPs) as well as Nafion nanocomposites at a 10 wt % loading of SiNPs (both annealed and unannealed membranes). A summary of the results of this analysis is presented in Table 1.

Note, a normalized relaxation time constant ($\beta_{norm} = L^2 \times \beta$) has been reported in Table 1 to allow for accurate comparison of relaxation time constants obtained from the analysis of

DOI: 10.1021/acsapm.9b00866
ACS Appl. Polym. Mater. 2020, 2, 40−54

membranes with different thicknesses. Briefly, as the time scale for water diffusion is thickness dependent, and as polymer relaxation is driven by the diffusion of water, we must correct the calculated polymer relaxation time constants by normalizing this parameter by the thickness of each membrane (i.e., scaling with the square of the thickness of the membrane).[43,47]

As seen from Table 1, the water diffusion coefficients range from $D = (5.7 \pm 2.4) \times 10^{-6}$ cm^2 s^{-1} for annealed Nafion containing 4 wt % SiNPs to $D = (22.4 \pm 4.3) \times 10^{-6}$ cm^2 s^{-1} for annealed, unmodified Nafion. There are a number of important things to highlight regarding the absolute magnitude of the diffusion coefficients reported in Table 1. First, the liquid water diffusivities we report here are up to five times higher than those previously reported for liquid water diffusion in extruded Nafion[24,29] and one to two orders of magnitude higher than those previously reported for water vapor diffusion in extruded Nafion 117 membranes (i.e., Nafion membranes with an equivalent weight = 1100 g/mol sulfonic acid).[23,24] In fact, this anomaly between liquid water and water vapor transport has been suggested as evidence of Schroeder's paradox as well as the presence of a water uptake "kinetic paradox". Further, it has been hypothesized that liquid water transport through these ionomers is faster due to the combined effect of the pressure head caused by the "reservoir" of water on top of the membranes and the fast reorganization of interfacial ionic moieties in the presence of liquid water, resulting in a more hydrophilic ionomer surface.[41] Further, it has also been posited that both faster liquid water transport and higher liquid water uptake are facilitated by the higher interconnectivity of ionic channels when these membranes are hydrated with liquid water.[26] Second, the calculated liquid water diffusion coefficient for annealed, unmodified Nafion is comparable to that of the self-diffusion coefficient of water ($\sim 2.6 \times 10^{-5}$ cm^2 s^{-1} at 25 °C).[48] According to the free-volume theory of diffusion,[49] diffusive motions of small solvent molecules are coupled to complementary movements of polymer segments to fill the voids left by the diffusing penetrant. A thermodynamic correlation between the mutual (or effective) diffusion coefficient (D, concentration gradient driven diffusion) and the self-diffusion coefficient (D_0) is found to be

$$D = AD_0 \exp\left[-\frac{E_A}{RT}\right] \tag{11}$$

where, A is a pre-exponential factor, which is a function of solvent activity, E_A is the activation energy of the diffusion process, R is the ideal gas constant, and T is the temperature of the system. In light of eq 11, this high water diffusion coefficient is quite surprising, as it suggests that the speed at which water diffuses through an initially dry, annealed Nafion membrane (diffusion driven by a chemical potential/concentration gradient) is analogous to the speed at which water molecules diffuse through bulk water (diffusion in the absence of a chemical potential/concentration gradient). As previously noted, water diffusion during this first sorption stage is expected to be impeded by the transition of the ionic network from a dry, partially collapsed state to that of a partially hydrated state,[26] underscoring that the diffusivities calculated from the kinetics of the first sorption stage are artificially high.

From Figure 4, it is clear that the concentration of water in the ionomer nanocomposite at the "pseudoequilibrium" of the first sorption stage is only a fraction of the total water concentration observed in the membrane at longer times ($t >$ 500 s). At early times, the membrane begins to equilibrate to the lower, local concentration of water present in the partially percolated ionic network rather than to the actual concentration of water associated with the presence of a liquid film at the polymer boundary. That is, the first water sorption stage only captures a partial hydration of the membrane, where more time is required for the membrane to become fully hydrated when exposed to liquid water. As such, the regression of the diffusion−relaxation model to the truncated time scale of the first water sorption stage results in the calculation of artificially high values of D. A quick back of the envelope calculation based on membrane thickness and the time it takes to reach the equilibrium plateau of the second sorption stage ($D = L^2/t_{eq} = (\sim 0.018\ \text{cm})^2/(\sim 150\ \text{s})$) gives a water diffusion coefficient of $\sim 2.1 \times 10^{-6}$ cm^2 s^{-1} (for annealed, unmodified Nafion), which falls well within the range of water diffusivities previously reported. While the diffusion coefficients reported herein are not quantitatively accurate, as they have been calculated based on the truncated experimental time scale of the first sorption stage, they provide a reasonable handle to study the observed changes to water transport in these ionomer nanocomposites as a function of the fabrication procedure.

Impact of Thermal Treatment and Presence of SiNPs.

From Table 1, it is evident that the introduction of SiNPs, as well as the heat treatment the ionomer receives, impacts both the liquid water diffusion through the membranes as well as the diffusion-induced ionomer relaxation kinetics. Comparing unmodified (i.e., no SiNPs) Nafion with and without thermal annealing, we see that thermal annealing results in almost a threefold increase in the calculated water diffusivity. Further, the normalized relaxation time constant for annealed Nafion membranes was about fourfold higher than that of their unannealed counterparts, indicating that the as-cast, unannealed Nafion is "stiffer". This result is counterintuitive, as annealing is expected to induce an enhanced ordering and chain packing in the Nafion microstructure (i.e., increased crystallinity), which should result in slower water sorption and polymer swelling kinetics.

Furthermore, thermal annealing is expected to constrain water uptake[40,50−52] by partially tying up (or "zipping") the ionomer matrix via formation of sulfonic anhydride within the ionic channels.[53,54] We have previously noted that this higher apparent stiffness for as-cast, unannealed membranes is most likely caused by the membrane fabrication method utilized for this experiment (i.e., solution casting), whereby the membranes are directly cast onto the ATR crystal.[20] In the as-cast state, the phase-segregated nanostructure of the unannealed membranes is assumed to be a nonequilibrium structure. That is, these unannealed membranes have not been provided with the necessary (thermal) energy to relax and rearrange into a less frustrated state. This assumption is based upon an exhaustive body of literature wherein other nanophase segregated block copolymers that have been fabricated using either spin or solution casting are observed to have a "frustrated-to-relaxed" transition when subjected to long thermal annealing.[55,56] The frustrated, nonequilibrium nanostructure of the unannealed Nafion results in both a lower water diffusivity and normalized relaxation time constant for these membranes. In contrast, the higher water diffusivity and faster polymer relaxation kinetics observed in annealed membranes may be attributed to the formation of a more

DOI: 10.1021/acsapm.9b00866
ACS Appl. Polym. Mater. 2020, 2, 40−54

ordered, fibrillar structure at the exposed ionomer surface, that readily reorganizes to conduct water molecules.[46,57] As the local nanostructure of the ionic domains influences transport through the membrane,[58] any disruption (or change) to these pathways can significantly alter the transport properties of the resulting membrane.

Next, a comparison of unannealed Nafion to its silica-incorporated counterpart provides direct insight into the impact of the SiNPs on water transport, as neither of these membranes has received thermal annealing. Interestingly, the water diffusivity increases by ≈100% with the introduction of 4 wt % SiNPs. This result indicates that the presence of the SiNPs enhances water transport through the unannealed nanocomposite. Enhanced water dynamics may be due to the formation of a more percolated ionic network in the presence of SiNPs, most likely via electrostatic interactions between the hydroxyl-rich NP surface and the sulfonic groups in Nafion.[7,11,32] Consequently, we observe an increase in the normalized relaxation time constant (≈150% increase) for the same sample.

Insight into the impact of both thermal annealing and SiNP incorporation on water transport can be obtained when we compare the water transport and swelling kinetics of unannealed and annealed Nafion membranes containing 4 wt % SiNPs. From Table 1, we observe that the calculated water diffusion coefficient and β_{norm} are reduced by ≈70 and ≈30%, respectively, when the Nafion membrane containing 4 wt % SiNP is annealed. Separately, consider the differences in the calculated values of D and β_{norm} for annealed Nafion membranes containing no SiNPs and those containing 4 wt % SiNPs. As seen in Table 1, the incorporation of SiNPs into annealed Nafion results in a reduction in both the swelling and water sorption kinetics (≈50% reduction in β_{norm} and ≈75% reduction in D). A combined overview of these results alludes to a synergistic effect of annealing and incorporation of SiNPs (at least at 4 wt %) into the ionomer, though it appears that annealing has a greater effect on water transport than the incorporation of the SiNPs. The addition of SiNPs in Nafion membranes has been shown to provide mechanical reinforcement to the ionomer matrix.[10,20,59,60] In fact, it is likely that SiNPs embedded in the matrix dissipate stresses more uniformly throughout the thickness of the film during hydration, resulting in a marked reduction in polymer swelling kinetics of annealed Nafion membranes with the introduction of 4 wt % SiNPs. Annealing the films results in the collapse of the ionic network, as all the water molecules are expelled and the sulfonic acid groups cross-link to form anhydride clusters.[52−54] Further, results from our previous study,[20] in conjunction with those reported by Di Noto and coworkers,[7,32] suggest that the SiNPs reside along the walls of the ionic channels (as a distinct inorganic phase) and may protrude into the channels. In this way, the hydroxyl-rich silica phase may facilitate the "zipping" of the ionic network in the dry ionomer via SiO_2−SO_3H interactions. This enhanced tying up of hydrophilic channels due to incorporation of SiNPs is immediately apparent from Table 1, where we see a 4-fold reduction in the diffusivity of water ($\sim 17 \times 10^{-6}$ vs $\sim 6 \times 10^{-6}$ $cm^2\ s^{-1}$) when Nafion membranes containing 4 wt % SiNPs are annealed.

However, this synergistic effect did not hold when the SiNP loading in the annealed Nafion membranes was increased from 4 to 10 wt %. The introduction of additional SiNPs resulted in approximate fourfold and twofold increase in the calculated water diffusion coefficient and normalized relaxation time constant, respectively. When the values of D and β_{norm} for annealed Nafion membranes containing no SiNPs and 10 wt % SiNPs are compared, we observe that the higher concentration of SiNPs in the 10 wt % membranes results in an ≈50% increase in relaxation kinetics, though interestingly, this increased concentration of SiNPs does not significantly impact the water sorption kinetics, as the calculated diffusivities for the two membranes are within ≈10% of each other. On the whole, these results are consistent with recent results from our group, where we conjectured that an increase in SiNP content within the membrane results in increased aggregation and growth of the inorganic phase into the hydrophobic matrix. Notably, previous work on proton dynamics in Nafion−SiNP membranes revealed similar results, where accelerated polymer and proton dynamics were observed in nanocomposites containing ≈9 wt % SiNPs. This result was attributed to a higher retention of water in these membranes due to the presence of the SiNPs,[7] which may also help explain the enhanced water transport and polymer swelling kinetics reported here when the NP loading is increased from 4 to 10 wt % in annealed membranes.

However, this appears to contradict the results regarding polymer swelling kinetics from our previous study, where the slowest water diffusion-induced swelling kinetics were observed for annealed, solution-cast Nafion membranes containing 10 wt % SiNPs. The discrepancy between the calculated swelling kinetics from our previous and present study is due to the shorter experimental time scales over which the swelling kinetics were characterized in the present study, i.e., the truncated time scale of the first water sorption stage. Multistage relaxation kinetics were not previously observed for annealed Nafion membranes containing 10 wt % SiNPs. This is attributed to lower temporal resolution of the previous *t*ATR-FTIR experiments as compared to the temporal resolution of the transport experiments presented here. In fact, even at significantly higher temporal resolution, the early time first stage in the uptake data for membranes containing 10 wt % SiNPs is quite faint (see Figure S6 in the Supporting Information). Without the presence of this first stage in the uptake data, the much longer experimental time scale (associated with the pseudoequilibrium of second sorption stage here) was considered, resulting in lower calculated values of D and β_{norm}.

Thus, by comparing changes in the water sorption and polymer swelling kinetics with the introduction of SiNPs as well as thermal treatment, the role of both these in governing water transport can be elucidated. First, the reduction of polymer swelling rate in Nafion−SiNP membranes indicates that these nanoparticles are interacting with the hydrophobic fluorocarbon matrix and affecting the thermomechanical behavior of the polymer at the nanoscale. The reinforcing effect of these interactions have been previously studied in various structure−property investigations, including ours.[7,10,20,32−34,59,60] Simultaneously, the hydrophilic surface of these nanoparticles impacts the connectivity/tortuosity of the ionic network through weak electrostatic interactions with the sulfonic groups. This dual action of SiNPs reflects in the synergistic impact of annealing and SiNP incorporation on the rate of first stage water transport, which is most inhibited for annealed Nafion nanocomposites with 4 wt % SiNPs. A nonlinear relationship between SiNP content and ionomer segmental mobility has been previously reported,[20,32] where

DOI: 10.1021/acsapm.9b00866
ACS Appl. Polym. Mater. 2020, 2, 40−54

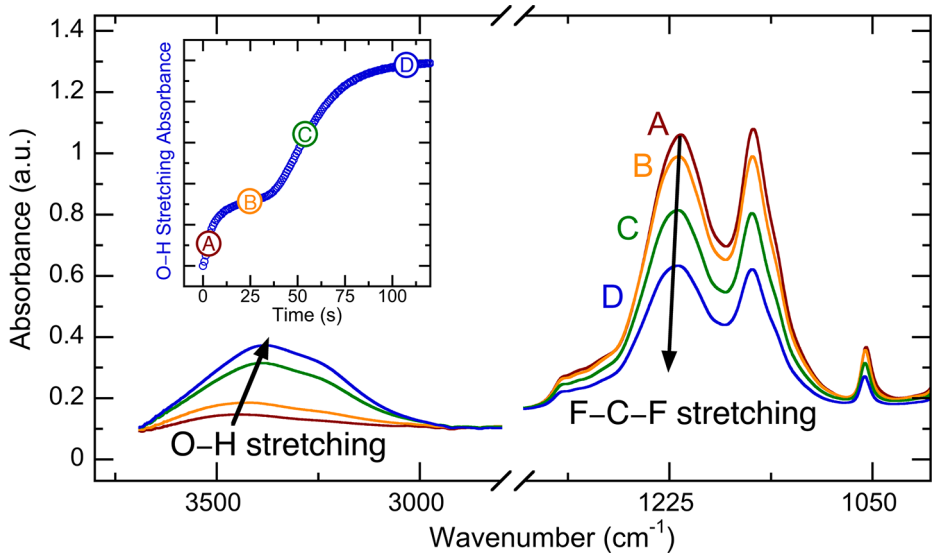

Figure 6. Spectra at selected time points showing shift in the O−H stretching peak over the course of a liquid water sorption experiment in annealed Nafion at 25 °C. Inset shows the time-resolved, two-stage water sorption kinetics for annealed, unmodified (i.e., 0 wt % SiNPs) Nafion, where the labels (A, B, C, and D) correspond to the time points at which the spectra shown in the larger figure were obtained.

SiNPs were found to hinder local fluorocarbon dynamics provided their concentration (with respect to the ion exchange capacity of the ionomer) remained below a "critical limit". However, above this critical limit, the ionomer dynamics were accelerated due to reduced participation of sulfonic groups in the formation of anhydrides in the dry ionomer nanocomposite. In addition, a study on the vanadium ion permselectivity of a series of Nafion−SiNP nanocomposites (prepared by the sol-gel method) found that the vanadium ion permeability decreased in the following manner: unannealed Nafion > annealed Nafion > annealed Nafion containing 10 wt % SiNPs.[2] The difference between the observed trends for water transport and vanadium ion between these studies underlines the need to elucidate both short-term and long-term water sorption processes in these ionomer nanocomposites.

To further quantify the coupling between diffusion (water sorption) and relaxation (polymer swelling), we invoke a dimensionless quantity known as diffusional Deborah number (De).[61] The Deborah number is defined as the ratio of the polymer relaxation time scale ($\tau_R = 1/\beta$) to the experimental time scale which, in our study, is represented by the time scale for diffusion ($\tau_D = L^2/D_{eff}$). That is, the diffusional Deborah number is calculated De = τ_R/τ_D. The magnitude of the diffusional Deborah number indicates the transport regime of the system, where De ≈ 1 is indicative of viscoelastic, anomalous (or non-Fickian) diffusion. The results of this analysis are presented in Table 1. As seen in Table 1, the calculated diffusional Deborah numbers for all membranes are De ∼ 1 (i.e., on the order of one), which is indicative of water diffusion and ionomer swelling occurring on similar time scales, confirming the anomalous, coupled diffusion−relaxation behavior observed in the *t*ATR-FTIR spectroscopy liquid water uptake data. Note, analysis of the Deborah number is limited by the fact that we are not capturing the complete time scale for both water diffusion and water-induced polymer relaxation. From Figure 4, it can be seen that the relaxation of fluorocarbon chains in Nafion not only continues during the second stage sorption process but also undergoes a transition, as the rate of polymer swelling increases with increased water sorption. However, based on our discussions above, analysis of the water uptake and polymer relaxation data through the lens of the Deborah number reflects the coupling between the water sorption kinetics and the viscoelastic response (for the first sorption stage), which we expect to be different from the second stage kinetics.

Origin of the Anomalous, Multistage Water Sorption Kinetics. To gain insight into the origins of the observed anomalous, multistage liquid water sorption kinetics, Figure 6 shows four IR spectra at distinct time points during initial hydration of a pristine, annealed Nafion membrane with liquid water. In Figure 6, Spectrum A was captured during the first water sorption stage, spectrum B was captured during the first stage pseudoequilibrium plateau, spectrum C was recorded during the second water sorption stage, and spectrum D was captured once the second stage "equilibrium" was attained. The time points associated with each of these spectra are highlighted in the inset in Figure 6. From Figure 6, we observe that the broad infrared band associated with the O−H stretching of water undergoes a red shift as the water sorption kinetics transition from the first to the second stage. The red shift of this infrared band is highlighted in Table 2, where the peak maximum of the broad O−H infrared band for spectra A−D is listed.

Further, we also observe the growth of an additional infrared band during the second water sorption stage, which can be seen as a more pronounced shoulder in the broad O−H stretching peak at lower wavenumbers. This additional infrared

Table 2. Location of the O−H Stretching Infrared Peak Maximum at Selected Time Points Along the Liquid Water Kinetic Curve for Annealed, Unmodified Nafion

selected time points from the liquid water kinetic data (−)	location of O−H stretching infrared peak maximum (cm^{-1})
during 1st sorption stage (spectrum A)	3444
at pseudoequilibrium (spectrum B)	3429
during 2nd sorption stage (spectrum C)	3390
at final equilibrium (spectrum D)	3382

DOI: 10.1021/acsapm.9b00866
ACS Appl. Polym. Mater. 2020, 2, 40−54

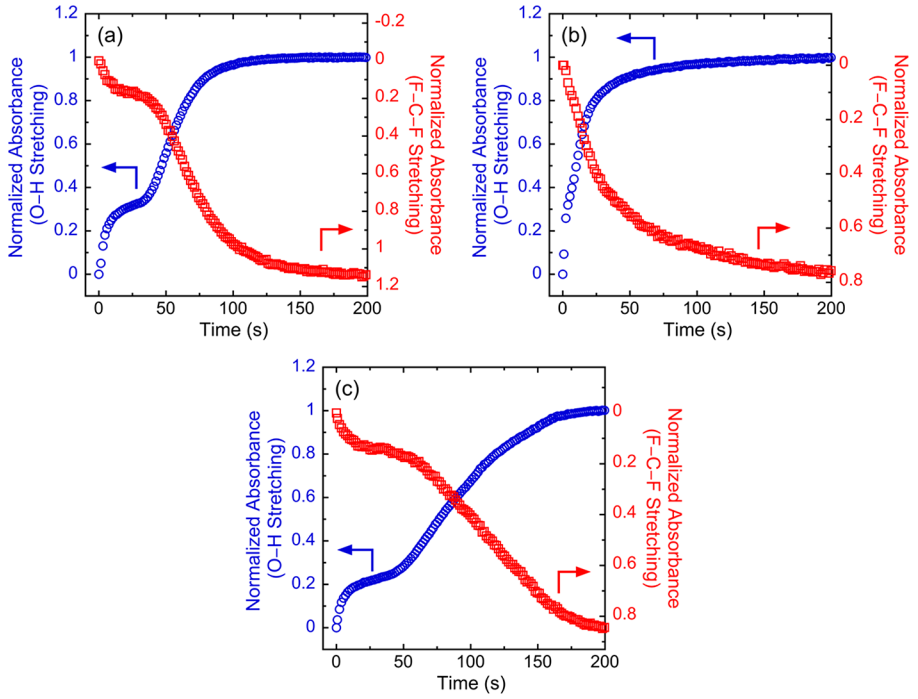

Figure 7. Normalized O−H stretching (open blue circles) and F−C−F stretching (open red squares) absorbance data as a function of time for liquid water diffusion in annealed, unmodified Nafion (i.e., no SiNPs) at 25 °C during the (a) initial hydration, (b) first rehydration after drying with high-purity nitrogen, and (c) second rehydration after reannealing the membrane at 140 °C for 2 h. Note, only 50% of the data are shown for clarity.

band is associated with the diffusion of strongly hydrogen bonded clusters of water molecules.[42] With this, it is apparent that the water molecules diffusing through the membrane during the first stage sorption are more strongly associated (or attracted) to the polar groups within the ionomer network and do not exhibit bulk water-like behavior. In contrast, the red shift of the broad O−H stretching peak as well as the emergence of a new infrared band is a result of the high degree of interaction between neighboring water molecules and is indicative of more bulk-like water transport.

To gain additional insight into the nature of the two-stage diffusion−relaxation process occurring in these membranes during hydration, a series of hydration-drying-rehydration experiments were performed. Figure 7 shows the normalized O−H stretching (open blue circles) and F−C−F asymmetric stretching (open red squares) absorbance data as a function of time for a series of hydration−drying−rehydration in annealed, unmodified Nafion (i.e., Nafion containing no SiNPs) at 25 °C. Specifically, Figure 7 shows the water uptake kinetics and polymer swelling kinetics of an annealed Nafion membrane during an initial hydration step and two additional rehydration steps with liquid water. For these experiments, the annealed Nafion film was exposed to liquid water during an initial hydration step (Figure 7a), after which the membrane was dried by flowing room temperature high-purity, dry nitrogen over the film. Following this drying step, the same membrane was again challenged with liquid water to perform a rehydration step (Figure 7b). Following this rehydration step, the membrane was not only dried using room temperature high-purity, dry nitrogen but was also reannealed at 140 °C for 2 h. After the membrane cooled to room temperature following reannealing, the same membrane was once again challenged with liquid water to perform a second rehydration step (Figure 7c).

As expected, in Figure 7a, two distinct stages are observed in the water uptake kinetic data and the polymer swelling kinetic data. The first of these steps approaches a pseudoequilibrium at approximately 30 s, after which the membrane continues to swell (open red squares) and continues to take up water (open blue circles). However, as seen in the transition from Figure 7a to Figure 7b, the two-stage water diffusion and polymer relaxation behavior vanishes once the Nafion membrane has undergone an initial hydration step with liquid water. The disappearance of the first water sorption stage with hydration and drying only with room temperature nitrogen begins to allude to the origins of that first stage being related to a local reorganization of the ionic network of the Nafion as it transitions from an initially dry to hydrated state. If the membrane is then dried at relatively low temperatures (e.g., room temperature nitrogen), the local ionic network formed during the initial hydration is not disrupted, as drying at such low temperatures does not drive off the tightly bound water molecules in the ionomer nor does it result in the formation of sulfonic anhydride cross-links within the ionic network.[29,57] Further, this result is consistent with recent work from Kusoglu et al.,[51] where they found that preconditioning the Nafion through hydration results in morphological ordering that is favorable for subsequent water sorption.

The notion that this first stage arises from a local reorganization of the ionic network is further supported by the fact that the two-stage water uptake and polymer swelling kinetics re-emerge once the membrane has undergone reannealing at 140 °C for 2 h (transition from Figure 7b to Figure 7c). Multiple studies have noted the reproducibility of a partially collapsed ionic network within Nafion upon annealing, which results in simultaneous expulsion of water molecules from the channels and formation of sulfonic anhydride.[53,54] These results further underscore the coupled

DOI: 10.1021/acsapm.9b00866
ACS Appl. Polym. Mater. 2020, 2, 40−54

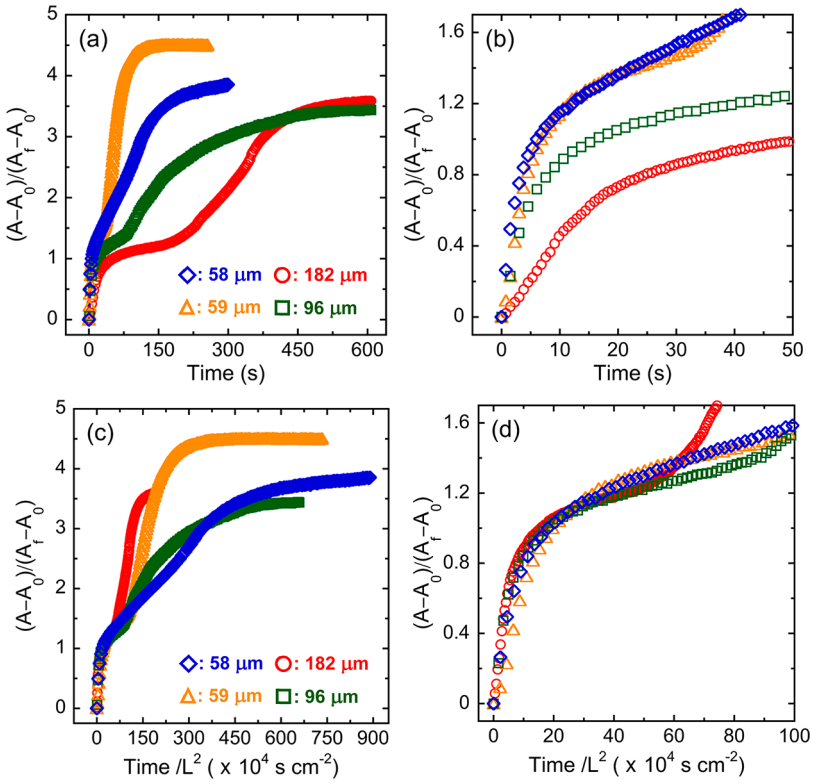

Figure 8. (a) Normalized, integrated O−H stretching absorbance data as a function of time for liquid water diffusion in annealed, unmodified Nafion at 25 °C for film thicknesses of 58 μm (open blue diamonds), 59 μm (open orange triangles), 96 μm (open green squares), and 182 μm (open red circles). (b) Enlarged view of the early time normalized, integrated O−H stretching absorbance data shown in panel a. Panels c and d are analogous to a and b, respectively, where the time axes have been normalized by the square of the membrane thicknesses.

nature of water diffusion and ionic network structure and the dynamics in these ionomer and ionomer nanocomposite membranes.

It is important to note that when discussing water transport in these solution-cast ionomer and ionomer nanocomposites, the experimental time and the membrane thickness are inherently coupled. That is, if the water uptake experiments shown in Figures 7a and 7c were conducted on a shorter time scale (t < 30 s) or were conducted on a thinner film, only a single water sorption and polymer swelling stage would have been observed. Therefore, it is important to adjust the experimental time to account for changes in membrane thickness to fully (and accurately) capture the water diffusion and polymer swelling behavior of these membranes.

To further illustrate this point, liquid water uptake experiments were performed on a series of unmodified, annealed Nafion membranes with thicknesses ranging from approximately 60 μm to approximately 190 μm. The results of this analysis are shown in Figure 8. Specifically, Figure 8a shows the normalized, integrated absorbance of the O−H stretching infrared band as a function of time for liquid water diffusion in annealed Nafion membranes of various thicknesses. Note, the data have been normalized to the first sorption stage pseudoequilibrium. To provide a more enhanced view of the first stage sorption process, the early time absorbance data (t < 100 s) have been highlighted in Figure 8b, where a pseudoequilibrium can be seen between 10 and 50 s for all membranes. From Figure 8a, two-stage water uptake kinetics is observed for all membrane thicknesses. As seen in Figure 8b, the water uptake data over this early time vary due to the difference in thicknesses among the annealed Nafion membranes. As the first sorption stage for all membranes is understood to emulate the previously mentioned diffusion−relaxation transport behavior, we expect that the effect of membrane thickness on the shape of the uptake kinetics of the first sorption stage can be removed by normalizing the time scale for each experiment by the thickness of the membrane.[37,38] Figures 8c and 8d show the same absorbance data from Figures 8a and 8b, respectively, where the absorbance data have now been plotted against experimental time divided by the square of the ionomer thickness. As seen from Figure 8d, when the absorbance data are plotted against a normalized experimental time scale, the first stage in the water uptake data for the various thicknesses collapse onto a single uptake curve at early normalized experimental times (<25 s cm^{-2}), after which the water uptake data for each membrane begin to deviate from one another. This observed incongruence between the different uptake curves during the second water sorption stage cannot be fully explained.

The nature of the transition from the first to the second sorption stage was further investigated by quantifying the time at which this transition occurs for membranes of varying thicknesses (hereafter referred to as “Stage 1 residence time”). The results of this analysis are presented in Figure 9. As seen in Figure 9, the Stage 1 residence time scales linearly with the film thickness of each sample. Note, at a film thicknesses of ∼60 μm, the membrane is close to a “critical film thickness” (calculated as ≈32 μm from Figure 9), where the transition between different sorption stages becomes indiscernible, and water sorption is observed to occur in a single stage. As such, for the two sorption curves presented for film thicknesses in

DOI: 10.1021/acsapm.9b00866
ACS Appl. Polym. Mater. 2020, 2, 40−54

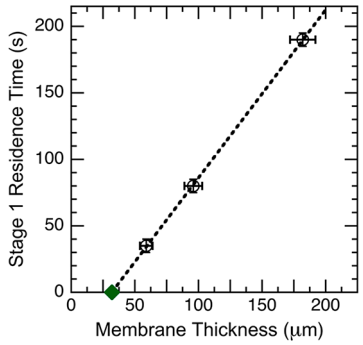

Figure 9. Stage 1 residence time as a function of film thickness for annealed, unmodified Nafion membranes. The dashed line represents the best-fit linear regression to the data. The solid green diamond at the *x*-intercept is the "critical thickness" of the film (≈32 μm) at which the plateau corresponding to the 1st sorption stage vanishes.

this range, the departure from first stage is slightly incongruent, and a clear transition from first stage to second stage is absent for the membrane with a thickness of 58 μm. Therefore, data from this film were not considered for this analysis.

Insights from Figures 6–9, in combination with key findings from previous investigations on liquid water transport in Nafion membranes,[21,25,27,40,62,63] help to elucidate the fundamental water transport mechanism governing the anomalous, multistage water sorption kinetics of these ionomer and ionomer nanocomposites. First, mathematically, both the first and second water uptake stages appear to have distinct origins. The first sorption stage (for a particular ionomer or ionomer nanocomposite) exhibits transport kinetics that scale with the square of membrane thickness, which indicates Fickian-like diffusion of water molecules during this first sorption stage. In contrast, the water uptake data for films with different thicknesses appear incongruent in the second sorption stage. However, the time at which the transition from the first to the second sorption stage occurs (Stage 1 residence time) is seen to be directly proportional to the film thickness, which indicates that the driving force behind this transition has a constant "rate of propagation" through the membranes. Second, chemically, based on the observed hydration–rehydration water uptake hysteresis as well as numerous reports on the chemical constitution of Nafion,[20,32,33,40,51−54] we conclude that the first water uptake stage, as seen for dry (thermally treated) Nafion and Nafion nanocomposites, is constrained by the local rearrangement of sulfonic acid groups in the partially hydrated ionic channels and by the growth of fully solvated ionic clusters.

From Figure 6 and Table 2, we identify the emergence of bulk-like transport of water molecules involved in the second water uptake stage. To complement our findings here, we consider a previous study regarding the evolution of water profiles across the thickness of Nafion 117 films, exposed to both liquid water and water vapor, with time.[27] In this study, transient liquid water transport through Nafion was found to occur via propagation of a liquid front through the ionomer.[27] Typically, such transport behavior is termed Case II or super-Case II diffusion.[25] The presence of a propagating liquid front may provide some explanation as to the origins of the full, multistage sorption curves we report in this study. Thus, the linear correlation between the Stage 1 residence time and film thickness becomes comprehensible if we consider a water transport model where, during membrane hydration, a liquid front follows a concentration gradient-driven diffusion regime. Thereby, the duration of the pseudoequilibrium of the first uptake stage is entirely governed by the speed at which the local ionic network can coalesce to form a fully hydrated and densely connected ionic network, after which the onset of the second uptake stage occurs and is independent of the local reorganizations of the ionic clusters. In other words, a liquid water layer propagates through the thickness of the membrane, swelling the ionic network and increasing interconnectivity, while a diffusion regime through the partially hydrated network precedes this front, creating a partially hydrated-percolated ionic network. Given this, the water diffusivity values extracted from this first water uptake stage should be viewed more as the speed at which water moves through the partially collapsed ionic network of the initially dry membrane and less as a measure of the speed at which the membrane reaches full hydration when challenged with liquid water. These insights are pivotal in the further development of a holistic transport model to describe liquid water sorption in Nafion and Nafion nanocomposites and can be valuable when trying to accurately model water diffusion through the membrane or even through membrane–electrode assemblies employed in fuel cells.[29]

CONCLUSION

In summary, we report, for the first time, the use of *t*ATR-FTIR spectroscopy to characterize liquid water transport and water diffusion-induced polymer relaxation kinetics in Nafion–SiNP membranes prepared via solution casting. The molecular-level resolution, combined with fast scan rates provided by this spectroscopic technique, allowed for the simultaneous capture of multistage water sorption and polymer swelling processes in real time. The first stage in the kinetic data was related to a fast polymer reorganization process, whereby the Nafion–SiNP membranes transitioned from a nonpercolated network to a hydrated, interconnected ionic network. It was found that this first sorption stage scales with the square of film thickness, suggesting that water transport during this early time is governed by a Fickian-like process. Further, hydration–rehydration experiments on the same samples confirm the intrinsic nature of this first stage process, which showed significant hysteresis over repeated hydration cycles.

However, we observed that reannealing the membranes after the first hydration resulted in the recovery of the multistage kinetic data captured for membranes undergoing initial hydration. Based on observations made in this work as well as the vast body of literature on water transport in Nafion, we posit that liquid water transport through dry Nafion membranes progresses in three stages: (1) quick (faster than time scales captured in these experiments) solvation of sulfonic groups; (2) diffusion of water molecules during a first stage swelling of ionic channels under moderate hydration; and (3) build-up and progression of a liquid water front behind the concentration gradient driven diffusion regime, wherein the ionic channels are fully hydrated and highly interconnected.

The swelling hysteresis and the dependence of the recovery of swelling behavior on thermal treatment is complementary to previous studies on the effect of pretreatment on the equilibrium properties of Nafion (such as net water uptake). In this way, this work helps to build a more comprehensive picture of water transport through perfluorosulfonated ionomers. The thickness-squared dependence of the first stage sorption kinetics suggests Fickian-like water transport during this water uptake stage, while the thickness dependence

DOI: 10.1021/acsapm.9b00866
ACS Appl. Polym. Mater. 2020, 2, 40−54

of the Stage 1 residence time indicates the presence of a liquid water front propagating through the membrane, analogous to Case II diffusion.

In the present study, the first stage sorption kinetics were regressed to a coupled diffusion−relaxation model, where both a liquid water diffusivity and normalized relaxation time constant were extracted from the analysis. Both these parameters were found to be impacted by incorporation of SiNPs as well as by thermal annealing. At low SiNP loadings, the introduction of SiNPs and thermal annealing exhibited a synergistic effect in Nafion−SiNP membranes, reducing the calculated D and β_{norm} by approximately 75% and 50%, respectively. In contrast, when the SiNP loading was increased to 10 wt %, the water sorption kinetics increased by almost 240% and was commensurate with that of water diffusion in annealed Nafion containing no SiNPs. We posit that the nonlinear relationship between nanoparticle loading and water transport as well as polymer swelling is indicative of the fact that the SiNPs do not reside within the ionic channels but instead reside at the hydrophobic−hydrophilic interface of the amorphous and ionic domains, where they primarily interact with sulfonic groups while also retaining water molecules on the interface. The highly coupled relationship between water diffusion and ionomer relaxation was further quantified using the dimensionless Deborah number. The Deborah number was found to be of the order of unity for all samples, signifying the concomitant nature of polymer swelling and water transport through these membranes. Results from this work provide the first molecular-level insights into the liquid water diffusion process in solution-cast Nafion and Nafion−SiNP membranes.

■ ASSOCIATED CONTENT

Supporting Information

The Supporting Information is available free of charge at https://pubs.acs.org/doi/10.1021/acsapm.9b00866.

Illustrative schematic of time-resolved ATR-FTIR spectroscopy experimental setup and time-resolved, normalized O−H stretching and F−C−F stretching absorbance data of liquid water diffusion in all membranes investigated in this work (PDF)

■ AUTHOR INFORMATION

Corresponding Author

*E-mail: ericd@clemson.edu.

ORCID

Apoorv Balwani: 0000-0001-8285-4787

Eric M. Davis: 0000-0002-5633-5489

Notes

The authors declare no competing financial interest.

■ ACKNOWLEDGMENTS

The authors gratefully acknowledge funding from the National Science Foundation under Award DMR-1848347. This work was also supported by Clemson University Department of Chemical and Biomolecular Engineering Start-Up Funds.

■ REFERENCES

(1) Parasuraman, A.; Lim, T. M.; Menictas, C.; Skyllas-Kazacos, M. Review of Material Research and Development for Vanadium Redox Flow Battery Applications. *Electrochim. Acta* **2013**, *101*, 27−40.

(2) Davis, E. M.; Kim, J.; Oleshko, V. P.; Page, K. A.; Soles, C. L. Uncovering the Structure of Nafion-SiO $_2$ Hybrid Ionomer Membranes for Prospective Large-Scale Energy Storage Devices. *Adv. Funct. Mater.* **2015**, *25* (26), 4064−4075.

(3) Jang, S. S.; Molinero, V.; Çağın, T.; Goddard, W. A. Nanophase-Segregation and Transport in Nafion 117 from Molecular Dynamics Simulations: Effect of Monomeric Sequence. *J. Phys. Chem. B* **2004**, *108* (10), 3149−3157.

(4) Zhang, H.; Zhang, H.; Li, X.; Mai, Z.; Wei, W. Silica Modified Nanofiltration Membranes with Improved Selectivity for Redox Flow Battery Application. *Energy Environ. Sci.* **2012**, *5* (4), 6299−6303.

(5) Schwenzer, B.; Zhang, J.; Kim, S.; Li, L.; Liu, J.; Yang, Z. Membrane Development for Vanadium Redox Flow Batteries. *ChemSusChem* **2011**, *4* (10), 1388−1406.

(6) Dresch, M. A.; Matos, B. R.; Fonseca, F. C.; Santiago, E. I.; Carmo, M.; Lanfredi, A. J. C.; Balog, S. Small-Angle X-Ray and Neutron Scattering Study of Nafion-SiO2 Hybrid Membranes Prepared in Different Solvent Media. *J. Power Sources* **2015**, *274*, 560−567.

(7) Ghassemzadeh, L.; Pace, G.; Di Noto, V.; Müller, K. Effect of SiO2 on the Dynamics of Proton Conducting [Nafion/(SiO2)X] Composite Membranes: A Solid-State 19F NMR Study. *Phys. Chem. Chem. Phys.* **2011**, *13* (20), 9327.

(8) Jiang, R.; Kunz, H. R.; Fenton, J. M. Composite Silica/Nafion® Membranes Prepared by Tetraethylorthosilicate Sol−Gel Reaction and Solution Casting for Direct Methanol Fuel Cells. *J. Membr. Sci.* **2006**, *272* (1), 116−124.

(9) Mauritz, K. A.; Warren, R. M. Microstructural Evolution of a Silicon Oxide Phase in a Perfluorosulfonic Acid Ionomer by an in Situ Sol-Gel Reaction. 1. Infrared Spectroscopic Studies. *Macromolecules* **1989**, *22* (4), 1730−1734.

(10) Miyake, N.; Wainright, J. S.; Savinell, R. F. Evaluation of a Sol-Gel Derived Nafion/Silica Hybrid Membrane for Proton Electrolyte Membrane Fuel Cell Applications: I. Proton Conductivity and Water Content. *J. Electrochem. Soc.* **2001**, *148* (8), A898−A904.

(11) Jansto, A.; Davis, E. M. Role of Surface Chemistry on Nanoparticle Dispersion and Vanadium Ion Crossover in Nafion Nanocomposite Membranes. *ACS Appl. Mater. Interfaces* **2018**, *10*, 36385−36397.

(12) Hickner, M. A. Water-Mediated Transport in Ion-Containing Polymers. *J. Polym. Sci., Part B: Polym. Phys.* **2012**, *50* (1), 9−20.

(13) Page, Kirt A.; Rowe, Brandon W.; Masser, Kevin A.; Faraone, Antonio The Effect of Water Content on Chain Dynamics in Nafion Membranes Measured by Neutron Spin Echo and Dielectric Spectroscopy. *J. Polym. Sci., Part B: Polym. Phys.* **2014**, *52* (9), 624−632.

(14) Spohr, E.; Commer, P.; Kornyshev, A. A. Enhancing Proton Mobility in Polymer Electrolyte Membranes: Lessons from Molecular Dynamics Simulations. *J. Phys. Chem. B* **2002**, *106* (41), 10560−10569.

(15) Robertson, C. G.; Roland, C. M. Glass Transition and Interfacial Segmental Dynamics in Polymer-Particle Composites. *Rubber Chem. Technol.* **2008**, *81* (3), 506−522.

(16) Gagliardi, S.; Arrighi, V.; Ferguson, R.; Telling, M. T. F. Restricted Dynamics in Polymer-Filler Systems. *Phys. B* **2001**, *301* (1), 110−114.

(17) Dura, J. A.; Murthi, V. S.; Hartman, M.; Satija, S. K.; Majkrzak, C. F. Multilamellar Interface Structures in Nafion. *Macromolecules* **2009**, *42* (13), 4769−4774.

(18) Damasceno Borges, D.; Gebel, G.; Franco, A. A.; Malek, K.; Mossa, S. Morphology of Supported Polymer Electrolyte Ultrathin Films: A Numerical Study. *J. Phys. Chem. C* **2015**, *119* (2), 1201−1216.

(19) Kusoglu, A.; Kushner, D.; Paul, D. K.; Karan, K.; Hickner, M. A.; Weber, A. Z. Impact of Substrate and Processing on Confinement of Nafion Thin Films. *Adv. Funct. Mater.* **2014**, *24* (30), 4763−4774.

(20) Balwani, A.; Faraone, A.; Davis, E. M. Impact of Nanoparticles on the Segmental and Swelling Dynamics of Ionomer Nanocomposite Membranes. *Macromolecules* **2019**, *52* (5), 2120−2130.

DOI: 10.1021/acsapm.9b00866
ACS Appl. Polym. Mater. 2020, 2, 40−54

(21) Majsztrik, P. W.; Satterfield, M. B.; Bocarsly, A. B.; Benziger, J. B. Water Sorption, Desorption and Transport in Nafion Membranes. *J. Membr. Sci.* **2007**, *301* (1), 93−106.
(22) Zawodzinski, T. A.; Springer, T. E.; Davey, J.; Jestel, R.; Lopez, C.; Valerio, J.; Gottesfeld, S. A Comparative Study of Water Uptake By and Transport Through Ionomeric Fuel Cell Membranes. *J. Electrochem. Soc.* **1993**, *140* (7), 1981−1985.
(23) Hallinan, D. T.; De Angelis, M. G.; Giacinti Baschetti, M.; Sarti, G. C.; Elabd, Y. A. Non-Fickian Diffusion of Water in Nafion. *Macromolecules* **2010**, *43* (10), 4667−4678.
(24) Hallinan, D. Transport in Polymer Electrolyte Membranes Using Time-Resolved FTIR-ATR Spectroscopy. *IDEA: DREXEL LIBRARIES E-REPOSITORY AND ARCHIVES*; Drexel University, 2009.
(25) Satterfield, M. B.; Benziger, J. B. Non-Fickian Water Vapor Sorption Dynamics by Nafion Membranes. *J. Phys. Chem. B* **2008**, *112* (12), 3693−3704.
(26) Zhao, Q.; Majsztrik, P.; Benziger, J. Diffusion and Interfacial Transport of Water in Nafion. *J. Phys. Chem. B* **2011**, *115* (12), 2717−2727.
(27) Hwang, G. S.; Parkinson, D. Y.; Kusoglu, A.; MacDowell, A. A.; Weber, A. Z. Understanding Water Uptake and Transport in Nafion Using X-Ray Microtomography. *ACS Macro Lett.* **2013**, *2* (4), 288−291.
(28) Devanathan, R.; Venkatnathan, A.; Dupuis, M. Atomistic Simulation of Nafion Membrane: I. Effect of Hydration on Membrane Nanostructure. *J. Phys. Chem. B* **2007**, *111* (28), 8069−8079.
(29) Fumagalli, M.; Lyonnard, S.; Prajapati, G.; Berrod, Q.; Porcar, L.; Guillermo, A.; Gebel, G. Fast Water Diffusion and Long-Term Polymer Reorganization during Nafion Membrane Hydration Evidenced by Time-Resolved Small-Angle Neutron Scattering. *J. Phys. Chem. B* **2015**, *119* (23), 7068−7076.
(30) Mauritz, K. A.; Stefanithis, I. D. Microstructural Evolution of a Silicon Oxide Phase in a Perfluorosulfonic Acid Ionomer by an in Situ Sol-Gel Reaction. 2. Dielectric Relaxation Studies. *Macromolecules* **1990**, *23* (5), 1380−1388.
(31) Stefanithis, I. D.; Mauritz, K. A. Microstructural Evolution of a Silicon Oxide Phase in a Perfluorosulfonic Acid Ionomer by an in Situ Sol-Gel Reaction. 3. Thermal Analysis Studies. *Macromolecules* **1990**, *23* (8), 2397−2402.
(32) Di Noto, V.; Gliubizzi, R.; Negro, E.; Pace, G. Effect of SiO2 on Relaxation Phenomena and Mechanism of Ion Conductivity of [Nafion/(SiO2)x] Composite Membranes. *J. Phys. Chem. B* **2006**, *110* (49), 24972−24986.
(33) Adjemian, K. T.; Dominey, R.; Krishnan, L.; Ota, H.; Majsztrik, P.; Zhang, T.; Mann, J.; Kirby, B.; Gatto, L.; Velo-Simpson, M.; Leahy, J.; Srinivasan, S.; Benziger, J. B.; Bocarsly, A. B. Function and Characterization of Metal Oxide−Nafion Composite Membranes for Elevated-Temperature H2/O2 PEM Fuel Cells. *Chem. Mater.* **2006**, *18* (9), 2238−2248.
(34) Antonucci, P. L.; Aricò, A. S.; Cretì, P.; Ramunni, E.; Antonucci, V. Investigation of a Direct Methanol Fuel Cell Based on a Composite Nafion®-Silica Electrolyte for High Temperature Operation. *Solid State Ionics* **1999**, *125* (1), 431−437.
(35) Shen, Y.; Wang, H.; Zhong, W.; Wu, P. Two-Dimensional ATR-FTIR Spectroscopic Study on the Water Diffusion Behavior in Polyimide/Silica Nanocomposite. *Chin. J. Chem. Phys.* **2006**, *19* (6), 481.
(36) Döppers, L.-M.; Breen, C.; Sammon, C. Diffusion of Water and Acetone into Poly(Vinyl Alcohol)−Clay Nanocomposites Using ATR-FTIR. *Vib. Spectrosc.* **2004**, *35* (1), 27−32.
(37) Davis, E. M.; Minelli, M.; Giacinti Baschetti, M.; Elabd, Y. A. Non-Fickian Diffusion of Water in Polylactide. *Ind. Eng. Chem. Res.* **2013**, *52* (26), 8664−8673.
(38) Davis, E. M.; Minelli, M.; Giacinti Baschetti, M.; Elabd, Y. A. Erratum: Non-Fickian Diffusion of Water in Polylactide. *Ind. Eng. Chem. Res.* **2014**, *53* (20), 8666−8666.
(39) Gebel, G.; Lyonnard, S.; Mendil-Jakani, H.; Morin, A. The Kinetics of Water Sorption in Nafion Membranes: A Small-Angle Neutron Scattering Study. *J. Phys.: Condens. Matter* **2011**, *23* (23), 234107.
(40) Zawodzinski, T. A.; Derouin, C.; Radzinski, S.; Sherman, R. J.; Smith, V. T.; Springer, T. E.; Gottesfeld, S. Water Uptake by and Transport Through Nafion® 117 Membranes. *J. Electrochem. Soc.* **1993**, *140* (4), 1041−1047.
(41) Rivin, D.; Kendrick, C. E.; Gibson, P. W.; Schneider, N. S. Solubility and Transport Behavior of Water and Alcohols in Nafion™. *Polymer* **2001**, *42* (2), 623−635.
(42) Pereira, M. R.; Yarwood, J. ATR-FTIR Spectroscopic Studies of the Structure and Permeability of Sulfonated Poly(Ether Sulfone) Membranes. Part 1.—Interfacial Water−Polymer Interactions. *J. Chem. Soc., Faraday Trans.* **1996**, *92* (15), 2731−2735.
(43) Davis, E. M.; Stafford, C. M.; Page, K. A. Elucidating Water Transport Mechanisms in Nafion Thin Films. *ACS Macro Lett.* **2014**, *3* (10), 1029−1035.
(44) Heitner-Wirguin, C. Infra-Red Spectra of Perfluorinated Cation-Exchanged Membranes. *Polymer* **1979**, *20* (3), 371−374.
(45) Kusoglu, A.; Modestino, M. A.; Hexemer, A.; Segalman, R. A.; Weber, A. Z. Subsecond Morphological Changes in Nafion during Water Uptake Detected by Small-Angle X-Ray Scattering. *ACS Macro Lett.* **2012**, *1* (1), 33−36.
(46) Goswami, S.; Klaus, S.; Benziger, J. Wetting and Absorption of Water Drops on Nafion Films. *Langmuir* **2008**, *24* (16), 8627−8633.
(47) Davis, E. M.; Benetatos, N. M.; Regnault, W. F.; Winey, K. I.; Elabd, Y. A. The Influence of Thermal History on Structure and Water Transport in Parylene C Coatings. *Polymer* **2011**, *52* (23), 5378−5386.
(48) Wang, J. H. Self-Diffusion Coefficients of Water. *J. Phys. Chem.* **1965**, *69* (12), 4412−4412.
(49) Wypych, G. *Handbook of Solvents*, 3rd ed.; ChemTec Publishing; Vol. *1*.
(50) Kusoglu, A.; Weber, A. Z. New Insights into Perfluorinated Sulfonic-Acid Ionomers. *Chem. Rev.* **2017**, *117* (3), 987−1104.
(51) Kusoglu, A.; Savagatrup, S.; Clark, K. T.; Weber, A. Z. Role of Mechanical Factors in Controlling the Structure−Function Relationship of PFSA Ionomers. *Macromolecules* **2012**, *45* (18), 7467−7476.
(52) Shi, S.; Dursch, T. J.; Blake, C.; Mukundan, R.; Borup, R. L.; Weber, A. Z.; Kusoglu, A. Impact of Hygrothermal Aging on Structure/Function Relationship of Perfluorosulfonic-Acid Membrane. *J. Polym. Sci., Part B: Polym. Phys.* **2016**, *54* (5), 570−581.
(53) Singhal, N.; Datta, A. Reversible Tuning of Chemical Structure of Nafion Cast Film by Heat and Acid Treatment. *J. Phys. Chem. B* **2015**, *119* (6), 2395−2403.
(54) Collette, F. M.; Thominette, F.; Mendil-Jakani, H.; Gebel, G. Structure and Transport Properties of Solution-Cast Nafion® Membranes Subjected to Hygrothermal Aging. *J. Membr. Sci.* **2013**, *435*, 242−252.
(55) Mori, K.; Hasegawa, H.; Hashimoto, T. Ordered Structure in Block Polymer Solutions: 6. Possible Non-Equilibrium Effects on Growth of Self-Assembling Structures. *Polymer* **1990**, *31* (12), 2368−2376.
(56) O'Shaughnessy, B.; Vavylonis, D. Non-Equilibrium in Adsorbed Polymer Layers. *J. Phys.: Condens. Matter* **2005**, *17* (2), R63−R99.
(57) Chomakova-Haefke, M.; Nyffenegger, R.; Schmidt, E. Structure Reorganization in Polymer Films of Nafion Due to Swelling Studied by Scanning Force Microscopy. *Appl. Phys. A: Solids Surf.* **1994**, *59* (2), 151−153.
(58) Li, J.; Wilmsmeyer, K. G.; Madsen, L. A. Hydrophilic Channel Alignment Modes in Perfluorosulfonate Ionomers: Implications for Proton Transport. *Macromolecules* **2008**, *41*, 4555−4557.
(59) Majsztrik, P. W. Mechanical and Transport Properties of Nafion® for PEM Fuel Cells; Temperature and Hydration Effects. PhD Thesis, Princeton University: Princeton, 2008.
(60) Ladewig, B. P.; Knott, R. B.; Hill, A. J.; Riches, J. D.; White, J. W.; Martin, D. J.; Diniz da Costa, J. C.; Lu, G. Q. Physical and Electrochemical Characterization of Nanocomposite Membranes of Nafion and Functionalized Silicon Oxide. *Chem. Mater.* **2007**, *19* (9), 2372−2381.

DOI: 10.1021/acsapm.9b00866
ACS Appl. Polym. Mater. 2020, 2, 40−54

(61) Vrentas, J. S.; Jarzebski, C. M.; Duda, J. L. A Deborah Number for Diffusion in Polymer-Solvent Systems. *AIChE J.* **1975**, *21* (5), 894−901.
(62) Romero, T.; Mérida, W. Water Transport in Liquid and Vapour Equilibrated Nafion™ Membranes. *J. Membr. Sci.* **2009**, *338* (1−2), 135−144.
(63) Duan, Q.; Wang, H.; Benziger, J. Transport of Liquid Water through Nafion Membranes. *J. Membr. Sci.* **2012**, *392−393*, 88−94.

DOI: 10.1021/acsapm.9b00866
ACS Appl. Polym. Mater. 2020, 2, 40−54